Measurements of the Gluon Contribution to the Nucleon Spin

S. Platchkov

DAPNIA/SPhN, CEA Saclay, 91191 Gif-sur-Yvette, France

Abstract. Where is the nucleon spin coming from? After more than 15 years of both experimental and theoretical efforts, the answer to this question is still unsatisfactory. It is now firmly established that the quarks alone account for only about 30% of the nucleon spin. The remaining 70% are expected to come partly from the parton orbital momentum and partly from the gluons. The contribution of the gluons ΔG to the nucleon spin is one of the major goals of the COMPASS collaboration at CERN. In COMPASS, the gluon spin distribution is determined by two different techniques, allowing four independent measurements. The first technique is based on Q^2 evolution of the nucleon polarized structure function. The statistical accuracy reached by COMPASS makes possible an indirect determination of the shape of ΔG, via a Next-to leading order QCD fit. The second technique relies on the Photon-Gluon Fusion process, in which two hadrons are detected in coincidence with the scattered muon. According to the type of hadrons detected and to the kinematical cuts applied, this technique leads to three independent measurements of ΔG. Within the experimental uncertainties, all measurements point to values of the gluon contribution to the nucleon spin which are either small in absolute value or compatible with zero.

1 Introduction

Understanding the origin of the nucleon spin has been a major goal for both theorists and experimentalists for more than two decades (see e.g. Ref. [1]). Since protons and neutrons are made out of quarks and gluons, one must be able to establish the relationship between the value of the nucleon spin and the spins of its constituents. The nucleon spin can be decomposed as follows:

$$\frac{1}{2} = \Delta\Sigma + \Delta g + L_q + L_g. \tag{1}$$

where one should keep in mind that gauge invariance plays a role for the separation into quark and gluon pieces. Here $\Delta\Sigma$ and ΔG are the contributions coming from the quarks and from the gluons respectively. The quark and gluons orbital momenta are denoted by L_q and L_g. In a naive, non-relativistic quark model, gluon and orbital momentum do not contribute, so one has: $1/2 = 1/2\Delta\Sigma$, i.e. all the nucleon spin is carried by the quarks. Relativistic effects also play a role, reducing the expectation value of the quark spin content to 0.60 - 0.75.

Experimentally, the spin structure of the nucleon can be accessed through deep-inelastic lepton scattering, with both the beam and the target being polarized. The

experimental asymmetry is then related to the spin-dependent structure function of the nucleon. The first experiments of this kind were performed at SLAC in the 70's. Double-spin asymmetries were clearly observed, but the statistical accuracy of the data remained limited. The data were significantly improved more than a decade later, by the EMC experiment at CERN. The experimental asymmetries were found to be smaller than expected, implying that in the framework of the Quark-Parton Model (QPM) the quark contribution to the proton spin is small.

When it became available, this result created a great surprise. Additional experiments were performed and numerous new calculations were made. Today, after a large theoretical and experimental effort, we know with a good accuracy that the quarks contribute for about 30% of the nucleon spin, the remaining part being shared between the gluons and the orbital momentum. The measurement of the gluon contribution to the nucleon spin is presently one of the major goals of the COMPASS experiment at CERN. Since the data taking start-up in 2002, the COMPASS collaboration published, or released, a number of new results. After a short description of the experimental set-up, I will focuss on the recent results from the COMPASS experiment, and more specifically on the gluon contribution to the nucleon spin.

2 The COMPASS experiment

The COMPASS set-up was designed [2] for beam energies of 100 to 200 GeV and physics processes in which in addition to the scattered beam particle, one or more outgoing particles are detected. The set-up (Fig. 1) is built around two large dipole magnets that define two consecutive spectrometers, suitable for large and small scattering angles respectively. Several types of tracking detectors are used to cover the various phase space regions: silicon and scintillating fibers, Micromegas and GEM micromesh detectors, large proportional and drift chambers. Particle identification
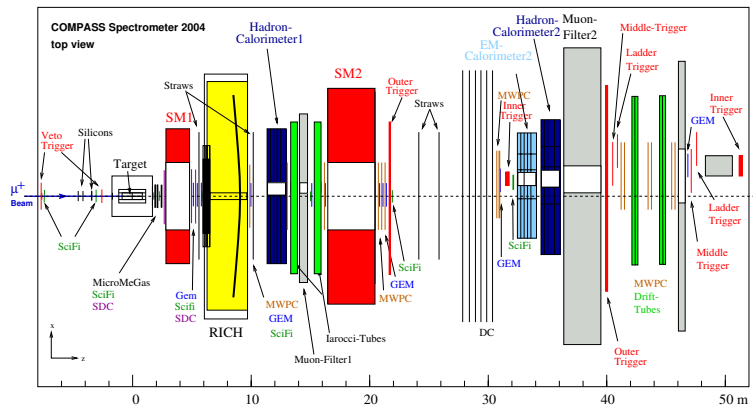
Figure 1. Top view of the Compass experimental set-up. The various detectors are indicated in the figure.

is performed using a RICH counter and both electromagnetic and hadron calorimeters. The polarized target (actually the largest polarized target in the world), consists of two oppositely polarized cells, $60\ cm$ long each, surrounded by a large solenoid superconducting magnet. Until 2006, the two cells were filled with a ^{6}LiD target material (mainly deuterium), for which polarizations better than 50% are routinely achieved. In 2007 we are using ammonia (NH$_3$, mainly proton), reaching polarizations of 90% and higher.

3 Lepton Scattering and the Spin-Dependent Structure Function

Polarized lepton scattering is the most straightforward tool for probing the spin structure of the nucleon. Within the Quark Parton Model (QPM), the incident lepton interacts with one and only one free quark in the nucleon. In the Deep Inelastic Scattering (DIS) limit the four-momentum transfer Q^2 and the energy transferred to the nucleon ν are large, but the ratio of these two quantities, the Bjorken scaling variable $x = Q^2/2M\nu$ remains constant. If we neglect the evolution with Q^2, which will be discussed below, the spin-dependent structure function of the nucleon g_1 is function of x only: $g_1 = g_1(x)$. Within the QPM one can write:

$$g_1(x) = \frac{1}{2} \sum_i e_i^2 \Delta q_i(x).$$ (2)

where $\Delta q_i(x)$ is the spin distribution for quarks of flavor i, as a function of x. If we take into account the antiquarks as well, and after integrating over the full region of x, we obtain the fraction $\Delta\Sigma$ of the nucleon spin carried by the quarks:

$$\Delta\Sigma = \int_0^1 dx \sum_i (\Delta q_i(x) + \Delta\bar{q}_i(x)).$$ (3)

The experimental observable is the double-spin lepton-nucleon asymmetry A_{exp}. Neglecting the small corrections coming form the transverse part of the asymmetry, A_{exp} is related to the virtual photon asymmetry A_1 through the relation:

$$A_{exp} \approx DP_BP_TfA_1,$$ (4)

where P_B and P_T are the beam and target polarizations respectively, f is the target dilution factor, and D is a kinematical factor. From A_1 one derives the spin structure function g_1:

$$g_1(x) \approx A_1(x)\frac{F_1(x)}{2x(1 + R(x))},$$ (5)

with $F_2(x)$ and R being the spin-averaged structure function and the ratio of the longitudinal to transverse photoabsorption cross sections respectively. Both quantities are well known from unpolarized DIS experiments.

Inclusive DIS cross section asymmetries were recently measured [3] at COMPASS for values of x ranging from 0.004 to 0.7 and for values of Q^2 between 1 and
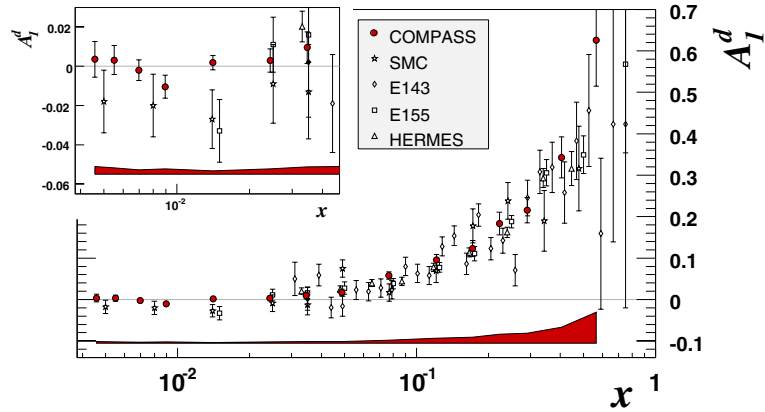
Figure 2. Experimental deuteron double-spin asymmetries The new COMPASS data are compared to previous results from SMC [4], HERMES [5] and SLAC [6, 7]. The shaded area indicates the systematic uncertainty of the COMPASS data. The insert is a zoom of the low-x region alone.

100 $(\text{GeV/c})^2$. The data are shown in Fig. 2. The asymmetries are in good agreement with previous data collected by SMC [4], HERMES [5], and the E143 and E145 experiments [6, 7] at SLAC. Two important observations can be made. First, the statistical improvement made by COMPASS is large, nearly an order of magnitude at small x. Second, the new data clearly show that for values of $x \leq 0.3$ the asymmetry is compatible with zero. This trend is further confirmed using the data with $Q^2 \leq 1$ $(\text{GeV/c})^2$, which covers the x domain down to values of 0.00004.
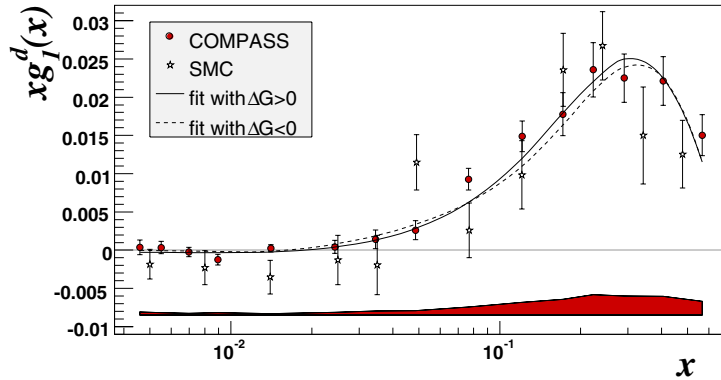
Figure 3. Deuteron polarized structure function $g_1^d(x)$. The shaded area indicates the systematic uncertainty of the COMPASS data. The curves show the two possible solutions for the QCD fits, with $\Delta G < 0$ and with $\Delta G > 0$.

4 Gluon spin distribution via a QCD analysis

The COMPASS deuteron spin structure function $g_1^d(x)$ is determined from the experimental asymmetries, using the formula 5 above. The resulting values are shown in Fig. 3 together with the results from SMC [4]. The curves are fits to the data, as described below.

The new COMPASS data are particularly precise and, for the first time, allow a sensible determination of all polarized parton distributions, including the gluon distribution. Since the Q^2-dependence for each bin of x is due to the scale evolution of the parton distributions, it can be used, through Next-to-Leading Order (NLO) perturbative QCD to determine the polarized gluon distribution itself. Several such fits have been performed in the past, see e.g. a recent one in Ref. [8].

In the QCD NLO fit the COMPASS data were combined with the proton, deuteron and ^{3}He data available (see Ref. [3] and references therein). The fit is performed using the QCD evolution equations, in which the Q^2 dependence of the nucleon polarized structure function is described in terms of singlet $\Delta\Sigma(x)$, non-singlet $\Delta q_3(x)$ and $\Delta q_8(x)$, and gluon $\Delta G(x)$ distributions. The fits are performed in the $\overline{MS}$ renormalization and factorization scheme and the parton distributions are taken at the reference Q_0^2 value of 3 (GeV/c)^2. In total, 230 data points were used, out of which 43 are from COMPASS.
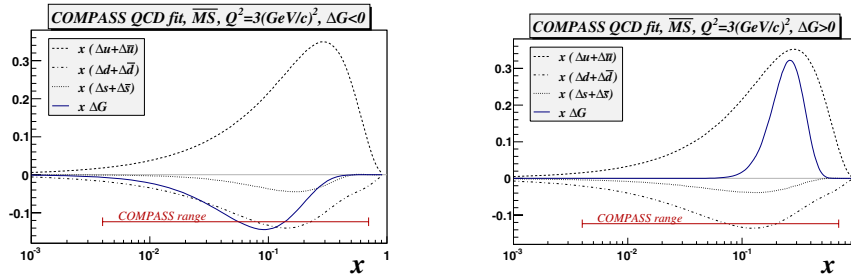
Figure 4. Parton distributions for the solutions $\Delta G < 0$ (left) and $\Delta G > 0$ (right).

Two different approaches for the fit were used: in the (x, Q^2) space [9] and in the space of moments [10] . Each of the two approaches arrives at two possiblities for the fit minima, one with $\Delta G < 0$ and the other with $\Delta G > 0$. In spite of the ΔG sign difference, the two fit results (displayed in Fig. 3, for one of the approaches only, the other approach gives nearly identical results) are hardly distinguishable all over the measured range in x. They also yield comparable $\Delta\Sigma(x)$, $\Delta q_3(x)$, and $\Delta q_8(x)$ distributions (Fig. 4) and have nearly identical χ^2 probabilities. The two fits start to differ only for the very low values of x and show an increasingly different behavior when x tends to zero. The first moments (integrals of $\Delta G(x)$) η_G for each of the two gluon distributions are small for both solutions and nearly equal in absolute values, i.e. $|\eta_G| \approx 0.2 - 0.3$. The quark contribution to the nucleon spin is: $\Delta\Sigma = 0.30 \pm 0.01(stat.) \pm 0.02(eval.)$ at the reference Q_0^2 of 3 (GeV/c)^2.
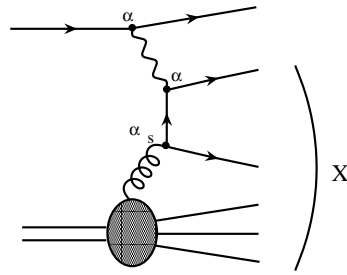
Figure 5. The Photon Gluon Fusion process. The virtual photon interacts with the gluon in the nucleon and creates a quark-antiquark pair. The strong and the electromagnetic coupling constants are indicated.

From the difference between $\Delta\Sigma(x)$ and $\Delta q_8(x)$ we also determine the strange quark distribution. It is negative, peaks at high x, and contributes to the nucleon spin for $\Delta s + \Delta\overline{s} = -0.10 \pm 0.01(stat.) \pm 0.01(evol.)$.

5 Gluon polarization from the Photon-Gluon Fusion process

The gluon polarization can be directly measured via the spin asymmetry of the Photon-Gluon Fusion (PGF) process. In this process the fusion of the virtual photon and the gluon creates a quark-antiquark pair in the final state (Fig. 5). The fragmenting quarks are then detected with two different, but complementary methods, providing three independent measurements of $\Delta G/G(x)$.

In the first method ("open charm") the charmed quark c hadronizes into a D^0 or a D^* meson. These mesons then decay into $K + \pi$ and $K + \pi + \pi_s$ hadrons respectively. Since this method is based on the detection of charmed quarks products, it has no contributions from channels involving the $u\bar{u}$, $d\bar{d}$ and $s\bar{s}$ quark pairs. Such a thorough selection insures that the c quarks are indeed created during the interaction. However, the corresponding counting rate is low, and the associated combinatorial background quite high.

In the second method, the PGF events are identified by requiring that two opposite-charge high-transverse momentum hadrons ("high-p_T pairs") are detected in coincidence. Since this method selects light quarks as well, its counting rate is high; however the competing processes involving e.g. resolved photon contributions, play a role and must be subtracted, introducing an additional model error in the results. As it will be discussed below, two kinematical domains can be selected, allowing for two independent measurements.

5.1 Open charm

The open charm channel selects a small but pure fraction of the PGF events, those originating from a charmed quark-antiquark pair. It is identified by the hadronic

modes of the decays $D^0 \to K^- \pi^+$ and $\bar{D}^0 \to K^+ \pi^-$. The background associated with the D^0 is particularly large; detection of the decays $D^{*+} \to D^0 \pi_s^+$ and $D^{*-} \to \overline{D}^0 \pi_s^-$ with π_s being a low-energy (soft) pion, significantly improve the signal over background ratio. This is illustrated in Fig. 6 for the D^* channel. The effective signals $S_{eff} = S/(1 + S/B)$ is also indicated.
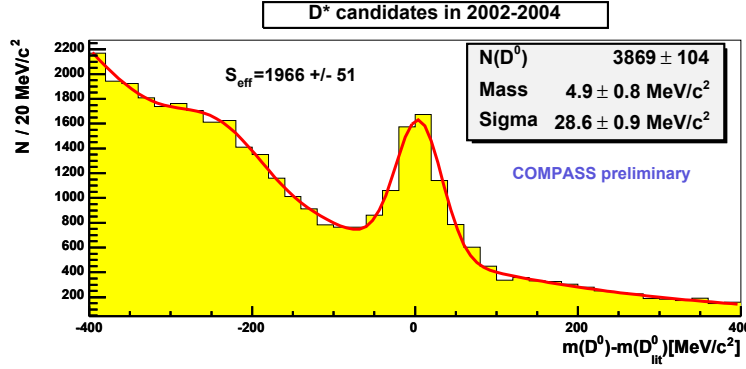
Figure 6. Invariant mass distribution in the D^* mass range as computed from the $D^* \to K\pi\pi_s$ candidates.

The gluon polarization is calculated from the experimental asymmetry using the relation:

$$A_{exp} = P_B P_T f a_{LL} \frac{S}{S + B} \Delta G/G, \tag{6}$$

where P_B and P_T are the beam and target polarizations respectively, f is the dilution factor, and $S/(S + B)$ the signal over background ratio. The analyzing power a_{LL} is calculated using a Monte-Carlo simulation. The resulting value of the gluon polarization obtained at $x_g = 0.15$ and for a scale of $\langle \mu^2 \rangle = 13$ (GeV/c)^2 is:

$$\Delta G/G(x_g) = -0.57 \pm 0.41 (stat). \tag{7}$$

5.2 High-p_T pairs

Contrary to the open charm, the high-p_T channel benefits from a much larger statistics. display The resulting Q^2 and the $\sum p_T^2$ experimental distributions are displayed in Fig. 7. However, large part of these events comes from background physics processes that are experimentally unknown. The corresponding contributions must be estimated using a Monte-Carlo simulation, on the expense of an additional model dependence in the result.

The relative amount of the background processes strongly depends on the Q^2 value of the data sample. For this reason the data were separated into two differents
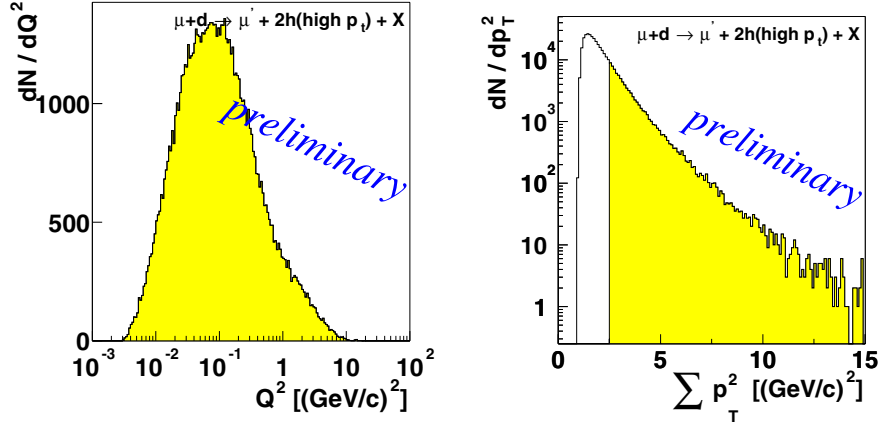
Figure 7. Measured distributions of Q^2 (left) and $\sum p_T^2$ (right) for high-p_T pairs. The data are separated into two sets, below and above Q^2=1 (GeV/c)^2.

sets and were analyzed independently. The first data set includes the high-p_T quasi-real photoproduction events with $Q^2 < 1$ (GeV/c)^2 only. In the second data set only the events with $Q^2 > 1$ (GeV/c)^2 were considered.

In the $Q^2 < 1$ (GeV/c)^2 region the dominant effect comes from the resolved photon contributions. These processes were simulated using the PYTHIA Monte-Carlo generator. It was found that the PGF events represent about 30% of the data sample and about half of the event number comes from the resolved photon processes. The simulation procedure and the resulting model errors are described in Ref. [11]. For the COMPASS data collected between 2002 and 2006, the result at $\langle x_g \rangle = 0.085$ and for $\langle \mu^2 \rangle = 0.085$ is:

$$\Delta G/G = 0.016 \pm 0.058(stat) \pm 0.055(syst). \qquad (8)$$

Here the systematic error includes both experimental and simulation systematics, the largest model error coming from the uncertainties on the Monte-Carlo parameters.

In contrast to the low Q^2 region, the background for the events with $Q^2 > 1$ (GeV/c)^2 is dominated by the leading and QCD-Compton processes. The corresponding contributions were estimated [11] using the LEPTO Monte-Carlo generator. After all cuts have been applied we obtain:

$$\Delta G/G = 0.06 \pm 0.31(stat) \pm 0.06(syst). \qquad (9)$$

for the COMPASS data collected in 2002 and 2003.

Fig. 8 shows the three COMPASS data points together with previous measurements from SMC [12] and HERMES [13]. The two QCD fit solutions for the $\Delta G/G(x)$ distribution, are also shown. The new COMPASS measurements are all compatible with both solutions, for the $\Delta G/G(x)$ distribution.
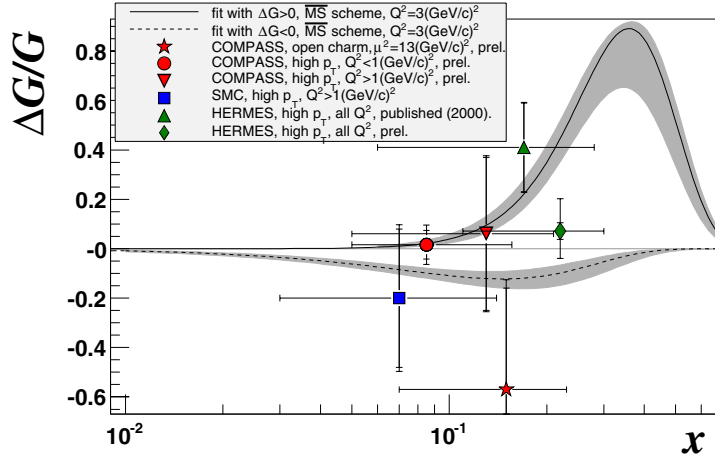
Figure 8. QCD fit results for the gluon distribution, together with the available $\Delta G/G$ measurements from COMPASS, SMC [12], and HERMES [13,14]

6 Measurements of the gluon polarization at HERMES and at RHIC

Studies of the gluon polarization observables were also undertaken at HERMES and at RHIC. The HERMES collaboration [14] used an incident positron energy of 27.5 GeV and an internal deuterium target. Charged inclusive high-p_T hadrons ($p_T > 1$ GeV/c) were detected in anti-coincidence with the beam particle. The PGF fraction was determined from the PYTHIA Monte Carlo code to be between 10% and 20% depending on p_T. The resulting $\Delta G/G$ value is:

$$\Delta G/G = 0.071 \pm 0.034(stat) \pm 0.010(syst). \tag{10}$$

The model dependence error is estimated to be 0.11. The new HERMES value is in good agreement with the results from COMPASS.

The gluon polarization is also being studied at the Brookhaven Relativistic Heavy Ion Collider (RHIC) by the PHENIX and the STAR collaborations. Using polarized proton-proton collisons these two collaborations are invstigating the gluon polarization with several methods. The statistically most significant method is the double spin asymmetry A_{LL} for π_0 or inclusive jet productions. The results of the 2005 run from the two collaborations show that the A_{LL} data is only compatible with calculations based on ΔG values of 0.5 or smaller. Once again, conclusions similar to those obtained by COMPASS can be drawn: large values of ΔG are excluded.

7 Conclusion

After nearly two decades of spin structure studies, the distribution of the polarized gluons in the nucleon starts to emerge. The accuracy of the latest inclusive data from COMPASS allows an indirect determination of $\Delta G(x)$. A QCD fit to the data yield two possible solutions for $\Delta G(x)$, either positive or negative. In both cases the absolute value of the first moment (or equivalently the gluon contribution to the nucleon spin) is small, of about 0.2-0.3. Large values of ΔG, such as advocated in the past for an explanation of the surprisingly small quark contribution, can be definitely excluded. The polarized gluon distribution was also measured directly, using the Photon-Gluon Fusion process. Three independent measurements by COMPASS, are available, and all of them are compatible with small values of $\Delta G(x)$. Good agreement with the latest data from HERMES and RHIC is obtained. The accuracy of the direct measurements is however not yet good enough to discriminate between the two possible solutions of the QCD fits.

References

1. S. Bass, *Rev. Mod. Phys. A* **77**, 1257 (2005).
2. P. Abbon, *et al.*, *Nucl. Instr. Meth. A* **577**, 455 (2007).
3. V. Alexakhin, *et al.*, *Phys. Lett. B* **647**, 330 (2007).
4. B. Adeva, *et al.*, *Phys. Lett. B* **420**, 180 (1998).
5. A. Airapetian, *et al.*, *Phys. Rev. D* **75**, 012003 (2005).
6. K. Abe, *et al.*, *Phys. Rev. D* **58**, 112003 (1998).
7. P. Anthony, *et al.*, *Phys. Lett. B* **463**, 339 (1999).
8. E. Leader, A. V. Sidorov and D. B. Stamenov, *Phys. Rev. D* **75**, 074027 (2007).
9. B. Adeva *et al.*, *Phys. Rev. D* **58** 112002 (1998).
10. A. N. Sissakian, O. Y. Shevshenko and O. N. Ivanov, *Phys. Rev. D* **70** 012002 (2004).
11. E. S. Ageev *et al.*, *Phys. Lett. B* **633** 25 (2006).
12. B. Adeva *et al.*, *Phys. Rev. D* **70** 012002 (2004).
13. A. Airapetian *et al.*, *Phys. Rev. Lett.* **84** 2584 (2000).
14. P. Liebing *et al.*, Contribution to DIS 2007, Munich, Germany, April 16-20 (2007).